Monolithic integrated-optic TDLAS sensors

Michael B. Frish[1 a], David R. Scherer[a], Richard T. Wainner[a], Mark G. Allen[a], Raji Shankar[b], Marko Lončar[b]
[a]Physical Sciences Inc., 20 New England Business Center, Andover, MA, USA 01810-1077,
[b]School of Engineering and Applied Sciences,
Harvard University, Cambridge, MA, USA 02138-2933

ABSTRACT

We are developing prototype chip-scale low-power integrated-optic gas-phase chemical sensors based on infrared Tunable Diode Laser Absorption Spectroscopy (TDLAS). TDLAS is able to sense many gas phase chemicals with high sensitivity and selectivity. Using semiconductor fabrication and assembly techniques, the low-cost integrated optic TDLAS technology will permit mass production of sensors that have wide ranging industrial, medical, environmental, and consumer applications. Novel gas sensing elements using low-loss resonant photonic crystal cavities or waveguides will permit monolithic integration of a laser source, sampling elements, and detector on a semiconductor materials system substrate. Practical challenges to fabricating these devices include: a) selecting and designing the high-Q micro-resonator sensing element appropriate for the selected analyte; and b) device thermal management, especially stabilizing laser temperature with the precision needed for sensitive spectroscopic detection. In this paper, we analyze the expected sensitivity of micro-resonator-based structures for chemical sensing, and demonstrate a novel approach for exploiting laser waste heat to stabilize the laser temperature.

Keywords: TDLAS, sensors, gas sensing, spectroscopy, integrated photonics, micro-resonator, photonic crystal cavity, quantum cascade laser

1. INTRODUCTION

Devices are needed to provide affordable, wide area chemical monitoring for quantitatively detecting trace gaseous chemicals, including Chemical Weapon Agents (CWAs) and Toxic Industrial Compounds (TICs). The ideal device will be: highly sensitive to and selective for the targeted chemical vapor with low false alarm rate; immune to electromagnetic interference and vibration; built ruggedly enough for dropping from an airplane; operable for at least several days when powered by self-contained batteries, and; so inexpensive that many hundreds or thousands of such sensors can be distributed cost-effectively over the area of interest and communicate among each other via a wireless network. Chip-scale low-power integrated-optic gas-phase chemical sensors based on the infrared laser technology generally known as Tunable Diode Laser Absorption Spectroscopy (TDLAS) can potentially address this need.[1]

Trace gas sensing and analysis by near-IR (NIR, 1.0 – 2.5 μm) TDLAS is a robust commercial technology capitalizing on reliable miniature distributed feedback (DFB) diode lasers that operate near room temperature.[2,3] TDLAS probes overtones of fundamental molecular rotational-vibration energy-state transitions, and can sense over a dozen simple molecules at ppm concentrations. Many of the more complex chemicals targeted by the envisioned sensors are spectrally active in the molecular fingerprint region of the midwave-infrared (MWIR, 3 -12 μm).[4-11] During the past decade, semiconductor quantum cascade lasers (QCLs) and interband cascade lasers (ICLs) have emerged as miniature industrial quality MWIR laser sources suitable for sensing these complex molecules, including TICs and CWAs.[12-13]

Advanced ICL and QCL laser technology is now yielding devices with thermal and power characteristics potentially suitable for the envisioned chip-scale TDLAS sensors.[14-17] Using semiconductor fabrication and assembly techniques, the low-cost integrated optic TDLAS technology envisioned herein will be an enabling advance in laser-based chemical sensing, permitting mass production of sensors that have wide ranging industrial, medical, environmental, and consumer applications. Each device will sense one targeted chemical; several devices working in tandem will sense several

[1]frish@psicorp.com; phone 1 978 689-0003; fax 1 978 689-3232; psicorp.com

chemicals. Novel gas sensing elements using solid-state optical waveguides will permit monolithic integration of a laser source, sampling element, and detector on a common substrate (Figure 1).

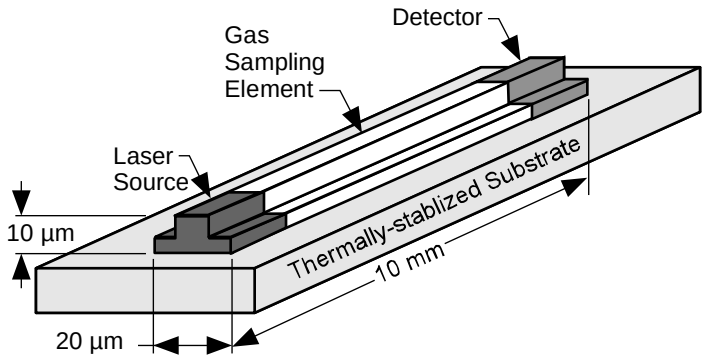

Figure 1. Schematic of monolithic sensor based on integration of a laser, sensing element (micro-resonator) and detector on a thermally-stabilized substrate.

This paper reports early steps towards this goal by addressing key technical issues inhibiting cost-effective integration on a monolithic platform: a) selecting sampling elements and detection modalities that provide the requisite sensitivity in configurations amenable to semiconductor fabrication; and b) minimizing the power consumed and discarded as waste heat to stabilize laser temperature. We theoretically evaluate the detection limits of potential sampling element designs based on state-of the-art photonic crystal structures coupled with MWIR Quantum Cascade Lasers (QCLs). We also demonstrate exploiting laser waste heat to stabilize the laser at an operating temperature above ambient, thereby virtually eliminating the power drawn by Peltier devices used traditionally to stabilize laser temperature.

2. SAMPLING ELEMENT DESIGN AND ANALYSIS

We envision a gas sampling element formed by a high-*Q* planar waveguide structure such as a photonic crystal (PhC) cavity or whispering-gallery-mode structure based on a micro-disk resonator. To enable volume production of an integrated device on a Si platform, we consider a Si MWIR PhC cavity[18] sensing element. Such a device provides a high *Q* in a small mode volume[19] and allows for monolithic integration with other components on a common substrate. As a specific example, we consider trace gas sensing of nitrous oxide (N_2O) in a Si PhC cavity at $\lambda = 4.46$ µm (2240 cm^{-1}), and analyze the expected sensitivity.

The relationship among cavity *Q*, resonance wavelength λ, and (intrinsic) cavity linewidth δλ, is $Q = \lambda/\delta\lambda$. Laser interrogation can measure with excellent precision both λ and δλ. Introducing an analyte into environment surrounding the resonant sensing element alters both the effective refractive index and the loss of the resonator, causing observable changes in λ and *Q*. In the discussion below, we compare the sensitivity based on measuring the resonance wavelength shift (referred to as refractive index sensing) with the change of cavity *Q* (referred to as direct absorption).

Refractive Index Sensing

Refractive index sensing is based on measuring the resonant wavelength shift, Δλ, resulting from small changes in the real part of the refractive index (RI) of the gas surrounding the sampling element.[20] The governing equation is:

$$\frac{\Delta\lambda}{\lambda} = \Gamma \frac{\Delta n}{n_{eff}} \tag{1}$$

where Γ is the overlap factor of the propagating waveguide or cavity mode with the analyte, Δn is the change in RI of the surrounding environment, and n_{eff} is the effective index of the propagating mode.[21]

The effective index n_{eff} depends on the fraction of the mode in the surrounding environment compared to the fraction in the Si structure:

$$n_{eff}^2 = \Gamma n_{gas}^2 + (1-\Gamma) n_{Si}^2 \tag{2}$$

where n_{gas} is the RI of the gas and n_{Si} is the RI of Si. The RI of the gas obeys the constitutive relationship:

$$n_{gas} = \eta n_{analyte} + (1-\eta) n_{air} \tag{3}$$

where η is the analyte concentration. Because the analyte concentration is very small, we can neglect terms of order η^2 and approximate n_{eff} as:

$$n_{eff}^2 = \Gamma n_{air}^2 + (1-\Gamma) n_{Si}^2 \tag{4}$$

After introduction of an analyte, the change in RI of the surrounding environment Δn can be written as:

$$\Delta n = n_{gas} - n_{air} = \eta\left(n_{analyte} - n_{air}\right) \tag{5}$$

This results in an analyte concentration η:

$$\eta = \frac{\Delta\lambda}{\lambda} \frac{n_{eff}}{\Gamma\left(n_{analyte} - n_{air}\right)} \tag{6}$$

Thus, the minimum detectable analyte concentration η_{min} is related to the minimum detectable shift in resonance wavelength Δλ according to Eq. (6).

To estimate an upper bound for the minimum detectable analyte concentration based on this sensing scheme, we assume that we can measure small changes in resonance wavelength Δλ to within a fraction of the cavity linewidth δλ according to $\Delta\lambda_{min} = F \cdot \delta\lambda$. We take an upper bound for $F \sim 10^{-2}$ based on an estimate of the laser linewidth with respect to cavity Q in the MWIR. Rewriting $\Delta\lambda_{min}$ as $\Delta\lambda_{min} = F\lambda/Q$, the minimum detectable concentration is:

$$\eta_{min} = \frac{F}{Q} \frac{n_{eff}}{\Gamma\left(n_{analyte} - n_{air}\right)} \tag{7}$$

Using $F = 10^{-2}$, $Q = 10^5$, Γ=0.5, $n_{air} = 1$, $n_{Si} = 3.42$, and $n_{analyte} = 1.000515$ for N_2O,[7] yields $\eta_{min,\,RI} \sim 1000$ ppm.

Direct Absorption

We now calculate the change in resonator Q based on direct absorption. The measureable Q, Q_{total}, is expressed as:

$$\frac{1}{Q_{total}} = \frac{1}{Q_{intrinsic}} + \frac{1}{Q_{analyte}} \tag{8}$$

where $Q_{intrinsic}$ is the Q in the absence of analyte and $Q_{analyte}$ describes the change induced by analyte.[22] The general relationship between Q and loss is:

$$Q = \frac{2\pi n_{eff}}{\alpha\lambda} \tag{9}$$

where the effective index of the mode is described above in Eq. (4) and α is the absorption coefficient (in units of cm^{-1}) of the gas. We modify the general expression of Eq. (9) to account for the modal overlap factor Γ and the gas concentration η,[23] resulting in:

$$Q_{analyte} = \frac{2\pi n_{eff}}{\Gamma\eta\alpha\lambda}, \tag{10}$$

and, using Eq. (10), re-write Eq. (8) as:

$$\delta\lambda_{Total} = \delta\lambda_{intrinsic} + \frac{\Gamma\eta\alpha\lambda^2}{2\pi n_{eff}} \tag{11}$$

Equation (11) expresses the total cavity linewidth as a sum of the intrinsic cavity linewidth and the change in linewidth (or, correspondingly, Q) of the cavity due to the introduction of analyte. As in the case for refractive index sensing, we express the upper bound to the limits for sensitivity as a fraction F of the intrinsic linewidth:

$$\delta\lambda_{min} = \frac{\Gamma\eta_{min}\alpha\lambda^2}{2\pi n_{eff}} = F \cdot \delta\lambda_{intrinsic} \tag{12}$$

Solving for η_{min} yields:

$$\eta_{min} = \frac{F}{Q_{intrinsic}} \frac{2\pi n_{eff}}{\lambda\Gamma\alpha} \tag{13}$$

Using $F = 10^{-2}$, $Q_{intrinsic} = 10^5$, Γ=0.5, λ=4.46μm, α=92cm^{-1}, yields $\eta_{min,direct}$ ~ 77 ppm. This is similar to the 100 ppm sensitivity demonstrated in a PhC slot waveguide for methane based on the direct absorption sensing modality.[24]

It is interesting to compare the final expressions for refractive index vs. direct absorption sensing. Re-arranging terms we can express Eqs. (7) and (13) as

$$\eta_{\mathrm{RI}} = \frac{\mathrm{F}n_{eff}}{Q\Gamma}\frac{1}{(n_{analyte}-n_{air})} \tag{14}$$

$$\eta_{\mathrm{direct}} = \frac{\mathrm{F}n_{eff}}{Q\Gamma}\frac{2\pi}{\alpha\lambda} \tag{15}$$

which highlights how these expressions scale with the real and imaginary parts of the complex refractive index, $N = n + i\kappa$, where $\kappa=\alpha\lambda/4\pi$.

3. LASER TEMPERATURE STABILIZATION

Current laser packages (e.g. Figure 2) utilize power-inefficient Peltier devices to maintain the laser temperature near 300 K (room temperature) with the ±10mK precision needed for sensitive gas detection. The laser and thermistor mount on a copper plate (the "sub-mount") on top of the Peltier device. Usually, the Peltier device is utilized as a thermoelectric cooler (TEC) to transport waste heat from the laser to a heat sink external to the laser package. To operate in this mode, power is supplied to the device. The voltage across the device determines the temperature difference between its upper and lower surfaces, and the current controls the rate of heat transfer. A feedback-controlled circuit that regulates the Peltier device voltage and current is commonly utilized to stabilize the thermistor temperature.

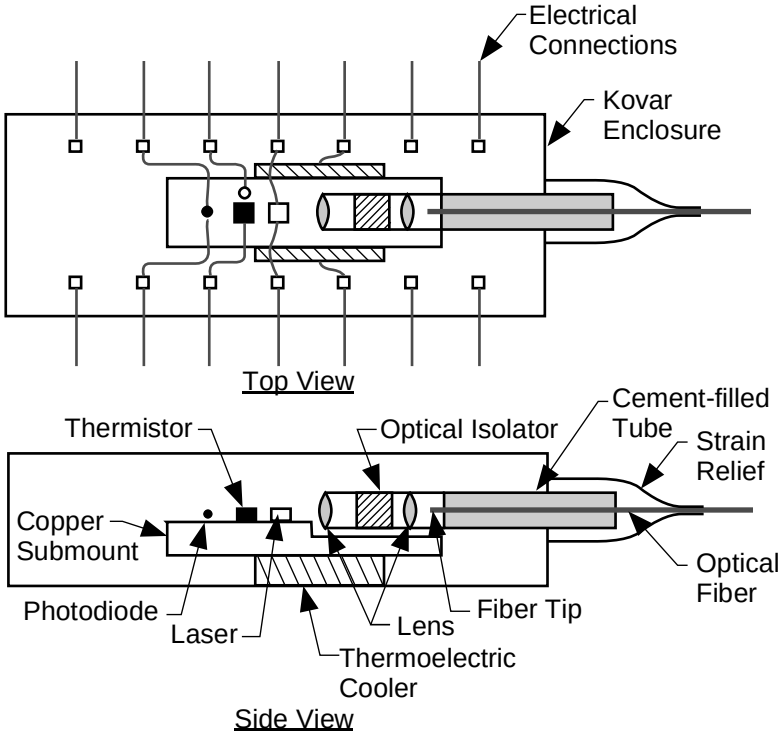

Figure 2. Telecommunications laser package, 14-pin butterfly style, with near-IR DFB laser.

The TEC is very inefficient; often, the tiny laser's waste heat is much less than the power demanded by the TEC itself to perform its function. In the low-power thermal stabilization concept, the objective is to *not* provide power to transport laser waste heat to a heat sink. Instead, waste heat raises the temperature of the laser (represented by thermistor temperature) to a stable operating point *above* ambient temperature. Precise temperature control is obtained by utilizing the Peltier device in a thermo-electric generation mode. Rather than supplying power to the device, we use it as a variable thermal conductor by installing a variable resistor across its electrodes. In this configuration, the temperature

difference created by heating the upper surface with laser waste heat creates a voltage across the electrodes (much like a thermocouple). The voltage drives a current through the resistor, thus dissipating power in the resistor. By controlling the resistance, the power dissipation is regulated. Providing feedback from the laser thermistor allows this technique to regulate and control the laser temperature, in principle with the same precision as actively cooling the laser with the Peltier device.

Demonstration with DFB Laser

To demonstrate this concept, we assembled an apparatus to measure the temperature difference created by the laser waste heat, as well as the voltage generated by the temperature difference, and demonstrated the ability to alter the temperature by adjusting the resistance across the Peltier electrodes. The apparatus uses a commercial laser controller with a NIR DFB laser installed. We disconnected the laser module's TEC pins (i.e. the electrodes for the Peltier device within the laser package). The controller provides utilities for measuring laser temperature, as well as the current and voltage that normally power the TEC to regulate laser temperature. These parameters are reported via a serial data link to a personal computer. Using a digital voltmeter (DVM) attached to the TEC leads, we measured the TEC voltage induced by the laser waste heat. In its voltage measurement mode, the resistance across the TEC leads is essentially infinite – the device acts as an open electrical circuit. Thus, it dissipates no heat through an external resistor, all of the laser waste heat is essentially dissipated by thermal conduction through the Peltier device. In contrast, when the DVM is in current measurement mode, its resistance is near zero and thus there can be little voltage across the Peltier electrodes. In this condition, the Peltier device cannot support a temperature difference across its surfaces and thus acts as a thermal conductor, transporting nearly all of the laser waste heat across the Peltier device to the heat sink, yet requiring no external power to do so (as if the laser was mounted directly on the heat sink).

Figure 3 shows laser temperature vs time with: a) laser, starting at ambient temperature, turned on from 0 mA to 120.2 mA with TEC leads short-circuited; b) Change from TEC short circuited to open-circuited; c) returned to short-circuited with laser current reduced to 90 mA; and d) current returned to 0 mA. The data show the anticipated behavior; with the laser off, the temperature is the same as ambient. With laser at high current (120 mA) and TEC short-circuited (period a), the laser temperature slowly rises above ambient and reaches a nearly steady value near 33.5 °C. Although the temperature difference across the TEC is small under this condition, heating the heat sink causes the laser temperature to rise above ambient. With TEC open circuited (period b), the laser temperature quickly rises above the heat sink temperature. Subsequently, the temperature decreases because the diminished thermal conductivity across the TEC allows the heat sink to cool.

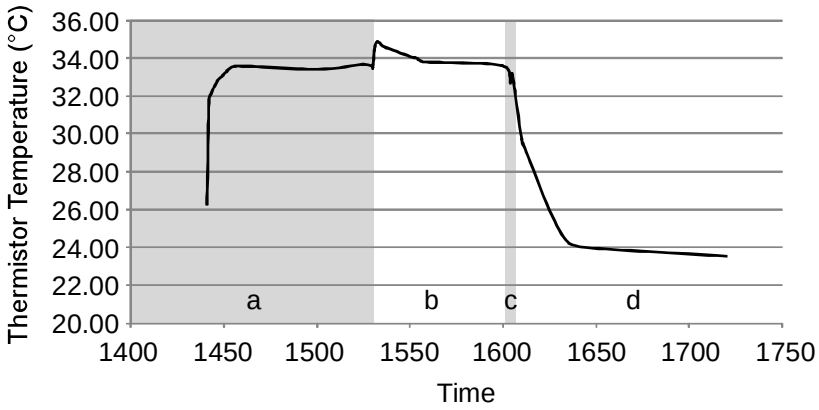

Figure 3. Laser temperature in various TEC configurations. a) laser startup at 120 mA with TEC leads short-circuited; b) TEC leads open-circuited; c) laser at 90 mA, TEC short-circuited; d) laser off, TEC short-circuited.

An alternate mode of operating with precise temperature control and little TEC power consumption is to set the laser temperature control point close to the value obtained with the TEC short circuited. Then, operating as a powered TEC, this temperature is obtained with little voltage, and thus little power, applied to the TEC. To demonstrate this mode, we measured TEC voltage, current, and power vs laser temperature at 120 mA laser current (Figure 4). These data show that indeed, the laser temperature can be stabilized above ambient while requiring essentially no TEC power. Notably, the operating temperature for minimum TEC power draw is about 32°C. Within the 2.5°C temperature setpoint resolution of these measurements, this value agrees with the temperature achieved with TEC electrodes shorted.

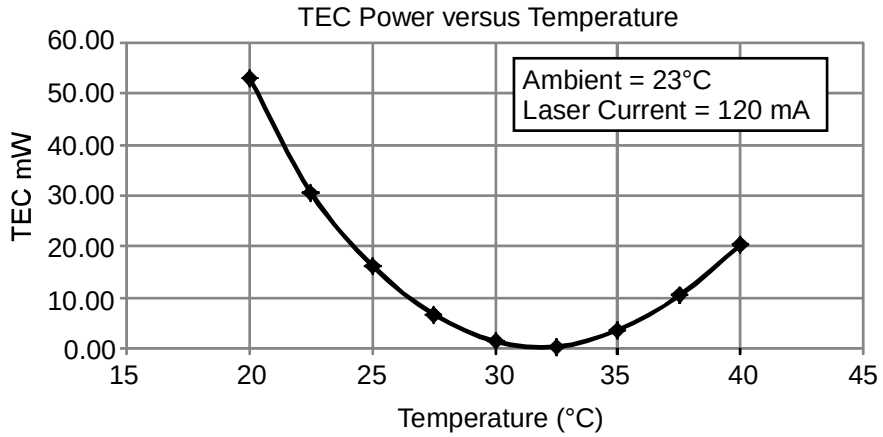

Figure 4. TEC power required to stabilize laser at selected temperature. Note that with virtually no power provided to the TEC, the laser stabilizes near 32°C.

Demonstration with Quantum Cascade Laser

We performed similar measurements using a singlemode mid-IR Quantum Cascade Laser (QCL), provided by Maxion Technologies, capable of operating at temperatures up to 50° C. Figure 5 plots TEC power vs temperature setpoint for a variety of laser currents. As with the DFB laser, for each laser current there is a corresponding temperature setpoint requiring essentially no TEC power. These results illustrate the capability to tune the laser wavelength by adjusting its current to achieve a desired temperature corresponding to the minimum TEC power draw for that current.

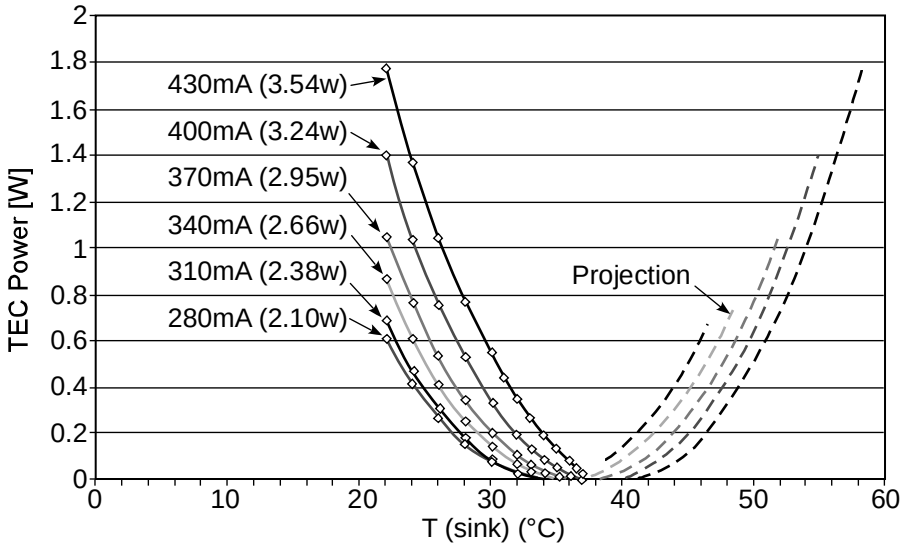

Figure 5. TEC power vs QCL submount temperature for several laser currents.

4. CONCLUSIONS

We have presented a theoretical comparison of two sensing modalities, refractive index sensing and direct absorption, for measuring trace chemical concentrations using micro-resonant photonic crystal cavity sensing elements in the MWIR. For the target analyte used in this study, N_2O, direct absorption (based on absorption of light associated with the imaginary part of the analyte's refractive index) is ~10X better than refractive index sensing (based on changes in the real part of the refractive index). The study, of course, does not yet consider effects of mechanical and thermal fluctuations on sensor performance.

We have also described a technique for minimizing the power wasted to stabilize laser temperature. Using the laser's waste heat to operate the laser at a temperature above ambient eliminates the need for traditional Peltier coolers.

5. ACKNOWLEDGMENT

This work has been sponsored by the US Army via SBIR Contract W911SR-11-C-0008. The authors thank Jim Jensen and Janet Jensen for their support.

REFERENCES

[1] M.B. Frish, R.T. Wainner, M.C. Laderer, B.D. Green, M.G. Allen, "Standoff and Miniature Chemical Vapor Detectors Based on Tunable Diode Laser Absorption Spectroscopy," IEEE Sensors Journal, Special Issue on Enhancement Algorithms, Methodologies and Technology for Spectral Sensing 10(3), 639-646 (2010).

[2] M.B. Frish, R.T. Wainner, M.G. Allen, W.J. Kessler, S.D. Wehe, M.C. Laderer, and B.D. Green, "The Evolution and Application of Trace Gas Analyzers based on Tunable Diode Laser Absorption Spectroscopy," Invited Presentation, *19th International Forum on Process Analytical Chemistry (IFPAC)*, Washington, DC (January 2005).

[3] M.A. Druy, M.B. Frish, and W.J. Kessler, "From Laboratory Technique to Process Gas Sensor - The Maturation of Tunable Diode Laser Absorption Spectroscopy," Spectroscopy 21(3), 14-18 (2006).

[4] M.G. Allen, D.J. Cook, B.K. Decker, J.M. Hensley, D.I. Rosen, M.L. Silva, and D.M. Sonnenfroh, "In-situ and stand-off sensing using QC/IC laser technology from 3 - 100 microns," Paper 5732-28, SPIE Integrated Optoelectronic Devices, Photonics West Conference, January, 2005.

[5] D.M. Sonnenfroh, E.W. Wetjen, M.G. Allen, C. Gmachl, F. Capasso, A.L. Hutchinson, D.L.Sivco, J.N. Baillargeon, and A.Y. Cho, "Mid-IR Gas Sensors Based on Quasi-CW Room-Temperature Quantum Cascade Lasers," Paper No. 2000-0641, AIAA 38th Aerospace Sciences Meeting, January 2000.

[6] A.A. Kosterev, F.K. Tittel, S.D. Wehe, D.M. Sonnenfroh, M.G. Allen, R. Kohler, C. Gmachl, F. Capasso, D.L. Sivco, and A.Y. Cho, "Spectroscopic trace gas detection with pulsed quantum cascade lasers," presented at the OSA Topical Meeting on Laser Applications to Chemical and Environmental Analysis, February 2002.

[7] I.G. Dunayevskiy, A. Tsekoun, M. Prasanna, R. Go, and C. Kumar N. Patel, "High-sensitivity detection of triacetone triperoxide (TATP) and its precursor acetone," Appl. Opt. **46**, 6397-6404 (2007).

[8] M.E. Webber, M.B. Pushkarsky and C. Kumar N. Patel, "Optical detection of chemical warfare agents and toxic industrial chemicals: Simulation," J. Appl. Phys. 97, 113101 (2005).

[9] M. Pushkarsky, A. Tsekoun, I.G. Dunayevskiy, R. Go and C. Kumar N. Patel, "Sub-parts-per-billion level detection of NO_2 using room temperature quantum-cascade lasers," Proceedings of the National Academy of Sciences 103, 10846-10849, (2006).

[10] C.M. Gittins, M.T. Boies, R.L. Coxe, B.K. Decker, J.M. Hensley, H.S. Kindle, D.C. Rossi, and M.G. Allen, "Remote sensing of chemical contamination using quantum cascade lasers," presented at the Solid State Lasers Technology Conference, June 2002.

[11] D.M. Sonnenfroh, M.B. Frish, R.T. Wainner, and M.G. Allen, "Mid-IR Quantum Cascade Laser Sensor for Tropospherically Important Trace Gases," Final Report prepared for U.S. Environmental Protection Agency under Order No. 4C-R348-NASA, PSI-2857/TR-1971, November 2004.

[12] S. Suchalkin, M. V. Kisin, Serge Luryi, and Gregory Belenky, F. J. Towner, J.D. Bruno, C. Monroy, and R. L. Tober, "Widely tunable type-II interband cascade laser," Appl. Phys. Lett. 8,031103 (2006).

[13] R. Q. Yang, J. L. Bradshaw, J. D. Bruno, J. P. Pham, D. E. Wortman, and R. L. Tober, "Room temperature type-II interband cascade laser," Appl. Phys. Lett. 81, 397 (2002).

[14] Liu, Z., Gmachl, C.F., Caneau, C.G., and Zah, C., "Very Small ($\leq$ 1.2 – 1.7 W) Heat Dissipation, Room Temperature, Continuous-Wave Quantum Cascade Lasers at $\lambda \sim 5.3$ μm," CLEO/QELS (2008).

[15] Y. A. Bakhirkin, A. A. Kosterev, G. Wysocki, F. K. Tittel, T. H. Risby, and J. D. Bruno, "Quantum cascade laser-based sensor platform for ammonia detection in exhaled human breath," in LACSEA OSA Technical Digest, Optical Society of America, (2008).

[16] R. Q. Yang, J. L. Bradshaw, J. D. Bruno, J. T. Pham, D. E. Wortman, "Power, Efficiency, and Thermal Characteristics of Type-II Interband Cascade Lasers", IEEE J. Quantum Electron. 37, 282 (2001).

[17] J. D. Bruno, J. L. Bradshaw, R. Q. Yang, J.T. Pham, D.Wortman, "Low-Threshold Interband Cascade Lasers with Power Efficiency Exceeding 9%," Appl. Phys. Lett. 76, 3167 (2000).

[18] R. Shankar *et al.*, "Mid-infrared photonic crystal cavities in silicon," Opt. Exp. 19(6) (2011).

[19] P.B. Deotare *et al.*, "High quality factor photonic crystal nanobeam cavities," Appl. Phys. Lett. 94, 121106 (2009).

[20] J.T. Robinson *et al.*, "On-chip gas detection in silicon optical microcavities," Opt. Exp. 16(6) (2008).

[21] J. Jagerska *et al*., "Refractive index sensing with an air-slot photonic crystal nanocavity," Opt. Lett. 35(15) (2010).
[22] M. Loncar *et al*., "Design and fabrication of photonic crystal quantum cascade lasers for optofluidics," Opt. Exp., 15(8) (2007).
[23] I.M. White and X. Fan, "On the performance quantification of resonant refractive index sensors," Opt. Exp., 16(2) (2008).
[24] W.-C. Lai *et al.*, "On-chip methane sensing by near-IR absorption signatures in a photonic crystal slot waveguide," Opt. Lett., 36(6) (2011).